

# Coherent energy loss effects in dihadron azimuthal angular correlations in Deep Inelastic Scattering at small $x$

Filip Bergabo<sup>1,2,\*</sup> and Jamal Jalilian-Marian<sup>1,2,†</sup>

<sup>1</sup>*Department of Natural Sciences, Baruch College, CUNY,  
17 Lexington Avenue, New York, NY 10010, USA*

<sup>2</sup>*City University of New York Graduate Center, 365 Fifth Avenue, New York, NY 10016, USA*

We perform an exploratory study of the role of coherent, medium-induced energy loss in azimuthal angular correlations in dihadron production in Deep Inelastic Scattering (DIS) at small  $x$  where the target proton/nucleus is modeled as a Color Glass Condensate. In this approach coherent radiative energy loss is part of the higher order corrections to the leading order dihadron production cross section. We include the effects of both gluon saturation and coherent radiative energy loss and show that radiative cold-matter energy loss has a significant effect on the so-called coincidence probability for the back to back production of dihadrons in DIS. We also define a double ratio of coincidence probabilities for a nucleus and proton targets and show that it is very robust against higher order radiative corrections.

## I. INTRODUCTION

The rise of parton (and especially gluon) distribution functions of a proton with decreasing Bjorken  $x$  as observed in Deep Inelastic Scattering (DIS) experiments at HERA [1] was a pleasant surprise which triggered intense theoretical and experimental studies of the behavior of QCD scattering cross sections at small  $x$  (equivalently, at high energy). This observed rise of the gluon distribution function can not however go on forever and must be tamed by high gluon density effects, the so-called gluon saturation [2, 3]. The color glass condensate (CGC) formalism [4] is an effective theory of high energy (or equivalently small  $x$ ) QCD which includes gluon saturation effects. In this formalism the small  $x$  gluon modes of a fast-moving proton or nucleus are collectively represented as a classical color field generated by the large  $x$  color degrees of freedom treated as static color charges [5, 6]. A high energy collision involving two hadrons/nuclei at small  $x$  in this approach is thus treated as a collision of two classical color fields, i.e. two color shock waves. On the other hand in DIS at small  $x$  one has a two-stage process where the virtual photon first splits into a quark anti-quark pair (a dipole) which subsequently scatter from the target hadron/nucleus modeled as a classical color field. Higher order loop corrections then lead to energy (equivalently  $x$  or rapidity) dependence of the quark anti-quark dipole-hadron/nucleus scattering cross section.

There have been numerous applications of the CGC formalism to particle production in high energy proton-proton, proton-nucleus and nucleus-nucleus collisions as well as to fully inclusive structure functions in DIS [7]. While there are strong hints for the presence of significant saturation effects in particle production spectra in the high energy hadronic and nuclear collisions at RHIC [8] and the LHC, more differential measurements in a cleaner environment [9] and higher precision theoretical calculations are needed to clearly establish gluon saturation as the dominant dynamics in the observed particle spectra at small  $x$ .

Two-particle production and azimuthal angular correlations are perhaps the most sensitive probe of saturation dynamics and as such have been intensively studied in the CGC formalism [10–23]. The Color Glass Condensate formalism predicts a broadening and eventual disappearing of the away side peak in dihadron back-to-back correlations [12] as experimentally observed in forward rapidity proton (deuteron)-nucleus collisions at RHIC [24, 25]. While Leading Order CGC calculations of dihadron production and angular correlations with (or without) running coupling corrections describe the experimental data quite well there may be other effects which also significantly contribute to this disappearance of the away side peak, for example, cold matter energy loss where one of the produced partons scatters from the nuclear target and radiates away some of its energy. Indeed it has been shown [26] that combining phenomenologically-motivated models of cold matter energy loss with models of nuclear shadowing of parton distribution functions can also describe the experimental data. Therefore it is prudent to understand how important cold matter energy loss effects are as compared with gluon saturation. It should be noted that the coherent energy loss as we define here is part of the Next to Leading Order (NLO) corrections to the Leading Order (LO) dihadron production cross section. In the Color Glass Condensate formalism this is true to any order in the coupling constant where the coherent energy loss is a higher order in  $\alpha_s$  correction to a fixed order calculation. Nevertheless as NLO corrections

\* fbergabo@gradcenter.cuny.edu

† jamal.jalilian-marian@baruch.cuny.edu

to this process [27] are not currently known<sup>1</sup> it is therefore useful to have a quantitative estimate of coherent energy loss effects on the dihadron azimuthal angular correlations.

In this exploratory work we study dihadron (quark anti-quark) azimuthal angular correlations in the back-to-back kinematics in DIS at small  $x$  where both gluon saturation and coherent cold matter energy loss are included using the same formalism. First, we re-derive the cross section for production of a quark, anti-quark and a gluon in DIS which was already done in [29, 30]. We then take the soft gluon limit and integrate over the final state gluon transverse momentum and compare the soft gluon radiation spectra, normalized to no radiation, between a nucleus and a proton target. Gaussian approximation is used to calculate the correlation functions of Wilson lines appearing as dipoles and quadrupoles which efficiently contain all the target information. We show that medium-induced coherent energy loss is most significant at the back to back limit and drops off as one goes away from this limit, and as one considers higher photon virtualities. We then consider the contribution of coherent energy loss to the away side peak in dihadron correlations in the back-to-back kinematics and show that it is significant. We then define a double ratio of coincidence probabilities and show that this double ratio is very robust against NLO corrections. We finish by outlining the steps needed for a more realistic study of medium-induced energy loss effects in dihadron angular correlations.

## II. COHERENT ENERGY LOSS IN DIS AT SMALL $x$ FROM CGC

The leading order process for dihadron<sup>2</sup> production in DIS at small  $x$  is the splitting of the virtual photon into a quark anti-quark pair which then multiply scatters on the target proton or nucleus. In the eikonal approximation inherent at small  $x$  it is assumed that the energy of the photon, and hence of the quark anti-quark pair, is so large that their recoil can be neglected and the pair stays on straight line trajectories while passing through the target. The scattering amplitude contains two Wilson lines [31] (multiple scatterings of each parton from the target is resummed into a Wilson line) so that dihadron production cross section involves not only dipoles but also quadrupoles, correlation functions of two and four Wilson lines. These dipoles and quadrupoles satisfy the BK/JIMWLK evolution equation [32–39] which governs their energy (rapidity or  $x$ ) dependence [40–42]. In the Color Glass Condensate formalism multiple scatterings and rapidity evolution result in the broadening and reduction of the away side peak in dihadron azimuthal angular correlations.

As either quark or anti-quark radiates a gluon, the energy carried away by the not-measured soft gluon will look as if it is lost in the process. Following Munier, Peigné and Petreska [43] we define the medium-induced radiation spectrum as

$$z_3 \frac{dI}{dz_3} = \frac{\frac{d\sigma^{\gamma^* A \rightarrow q\bar{q}gX}}{d^2\mathbf{p} d^2\mathbf{q} dy_1 dy_2 dy_3}}{\frac{d\sigma^{\gamma^* A \rightarrow q\bar{q}X}}{d^2\mathbf{p} d^2\mathbf{q} dy_1 dy_2}}. \quad (1)$$

where  $y_1, y_2, y_3$  are rapidities of the quark, anti-quark and radiated gluon respectively while  $\mathbf{p}, \mathbf{q}$  are the transverse momenta of the quark and anti-quark and the transverse momentum of the gluon is integrated over. Here  $z_3$  is the radiated gluon's fraction of the photon's plus momentum. We note that the three-parton production cross section in DIS at small  $x$  is already computed in [29, 30]. Integrating over the gluon momentum gives the contribution of the real corrections in the Next to Leading Order corrections to the Leading Order quark anti-quark production in DIS at small  $x$ . The medium-induced coherent energy loss is then defined [43] as the difference in radiation spectra between a nucleus and a proton target,

$$z_3 \frac{dI_{\text{ind}}}{dz_3} \equiv z_3 \frac{dI_A}{dz_3} - z_3 \frac{dI_p}{dz_3} = \frac{\frac{d\sigma^{\gamma^* A \rightarrow q\bar{q}gX}}{d^2\mathbf{p} d^2\mathbf{q} dy_1 dy_2 dy_3}}{\frac{d\sigma^{\gamma^* A \rightarrow q\bar{q}X}}{d^2\mathbf{p} d^2\mathbf{q} dy_1 dy_2}} - \frac{\frac{d\sigma^{\gamma^* p \rightarrow q\bar{q}gX}}{d^2\mathbf{p} d^2\mathbf{q} dy_1 dy_2 dy_3}}{\frac{d\sigma^{\gamma^* p \rightarrow q\bar{q}X}}{d^2\mathbf{p} d^2\mathbf{q} dy_1 dy_2}}. \quad (2)$$

where an integration over the transverse momentum of the radiated gluon is implied in the numerators.

Suppression of the away side peak in two-particle correlations as a function of the azimuthal angle  $\Delta\phi$  between the two outgoing particles in forward rapidity deuteron-nucleus collisions was predicted in [12] using leading order calculations of the coincidence probability  $\text{CP}(\Delta\phi)$ , here defined as [13],

<sup>1</sup> As this manuscript was being finalized we became aware of a very recent NLO calculation of dijet production [28].

<sup>2</sup> Everywhere in this paper we will consider partons rather than hadrons in the final state.

$$\text{CP}(\Delta\phi) = \frac{N_{\text{pair}}(\Delta\phi)}{N_{\text{trig}}}, \quad N_{\text{pair}}(\Delta\phi) = \int_{p_{\text{min}}}^{p_{\text{max}}} p \, dp \int_{q_{\text{min}}}^{q_{\text{max}}} q \, dq \frac{d\sigma^{\gamma^* A \rightarrow q\bar{q}X}}{d^2\mathbf{p} \, d^2\mathbf{q} \, dy_1 \, dy_2}, \quad N_{\text{trig}} = \int_{p_{\text{min}}}^{p_{\text{max}}} p \, dp \frac{d\sigma^{\gamma^* A \rightarrow qX}}{d^2\mathbf{p} \, dy_1}. \quad (3)$$

for dihadron production in DIS.  $\text{CP}(\Delta\phi)$  is a commonly studied observable which represents the probability per unit angle for correlated production of two hadrons; a leading (trigger) hadron with transverse momentum  $|\mathbf{p}|$  between  $p_{\text{min}}$  and  $p_{\text{max}}$  accompanied by an away side hadron with transverse momentum  $|\mathbf{q}|$  between  $q_{\text{min}}$  and  $q_{\text{max}}$  with an azimuthal angular separation of  $\Delta\phi$ . We will explore the contribution of fully coherent cold matter energy loss to  $\text{CP}(\Delta\phi)$  by adding radiative corrections to  $N_{\text{pair}}$  while using the leading order result for  $N_{\text{trig}}$ . In this preliminary study we will assume fixed rapidities to simplify our calculations.

We use the spinor helicity methods to calculate the quark anti-quark and quark anti-quark gluon production amplitudes. In the latter case there are four diagrams corresponding to the four possibilities when the gluon is radiated from either the quark or anti-quark and before or after the scattering from the target (see [30] for more details),

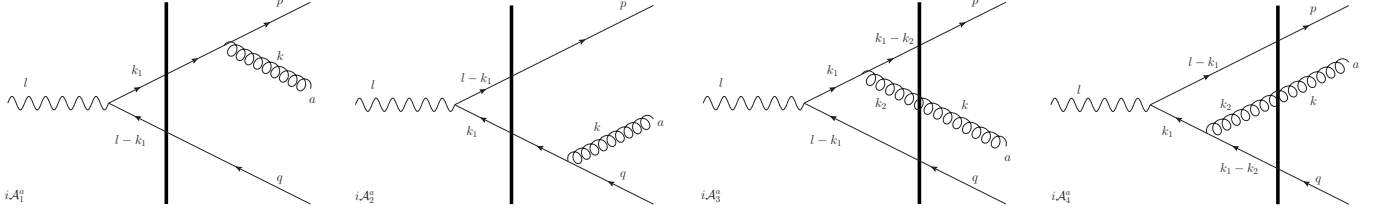


FIG. 1: The four diagrams for three parton production  $\gamma^* A \rightarrow q\bar{q}gX$ . The solid vertical line represents multiple scatterings from the target.

which can be evaluated to give

$$\begin{aligned} i\mathcal{M}_1^a &= 8egl^+ \int d^2\mathbf{x}_1 d^2\mathbf{x}_2 t^a V(\mathbf{x}_1) V^\dagger(\mathbf{x}_2) \int \frac{d^2\mathbf{k}_1}{(2\pi)^2} \frac{N_1 e^{i\mathbf{k}_1 \cdot (\mathbf{x}_1 - \mathbf{x}_2)} e^{-i(\mathbf{p} + \mathbf{k}) \cdot \mathbf{x}_1} e^{-i\mathbf{q} \cdot \mathbf{x}_2}}{\mathbf{k}_1^2 + z_2(1 - z_2)Q^2}, \\ i\mathcal{M}_2^a &= 8egl^+ \int d^2\mathbf{x}_1 d^2\mathbf{x}_2 V(\mathbf{x}_1) V^\dagger(\mathbf{x}_2) t^a \int \frac{d^2\mathbf{k}_1}{(2\pi)^2} \frac{N_2 e^{i\mathbf{k}_1 \cdot (\mathbf{x}_2 - \mathbf{x}_1)} e^{-i(\mathbf{q} + \mathbf{k}) \cdot \mathbf{x}_2} e^{-i\mathbf{p} \cdot \mathbf{x}_1}}{\mathbf{k}_1^2 + z_1(1 - z_1)Q^2}, \\ i\mathcal{M}_3^a &= \frac{8egl^+}{z_1} \int d^2\mathbf{x}_1 d^2\mathbf{x}_2 d^2\mathbf{x}_3 V(\mathbf{x}_1) t^b V^\dagger(\mathbf{x}_2) U(\mathbf{x}_3)^{ba} \int \frac{d^2\mathbf{k}_1}{(2\pi)^2} \frac{d^2\mathbf{k}_2}{(2\pi)^2} \frac{N_3 e^{i\mathbf{k}_1 \cdot (\mathbf{x}_1 - \mathbf{x}_2)} e^{i\mathbf{k}_2 \cdot (\mathbf{x}_3 - \mathbf{x}_1)} e^{-i\mathbf{k} \cdot \mathbf{x}_3} e^{-i\mathbf{p} \cdot \mathbf{x}_1} e^{-i\mathbf{q} \cdot \mathbf{x}_2}}{[\mathbf{k}_1^2 + z_2(1 - z_2)Q^2] \left[ Q^2 + \frac{\mathbf{k}_1^2}{z_2} + \frac{\mathbf{k}_2^2}{z_3} + \frac{(\mathbf{k}_1 - \mathbf{k}_2)^2}{z_1} \right]}, \\ i\mathcal{M}_4^a &= \frac{8egl^+}{z_2} \int d^2\mathbf{x}_1 d^2\mathbf{x}_2 d^2\mathbf{x}_3 V(\mathbf{x}_1) t^b V^\dagger(\mathbf{x}_2) U(\mathbf{x}_3)^{ba} \int \frac{d^2\mathbf{k}_1}{(2\pi)^2} \frac{d^2\mathbf{k}_2}{(2\pi)^2} \frac{N_4 e^{i\mathbf{k}_1 \cdot (\mathbf{x}_2 - \mathbf{x}_1)} e^{i\mathbf{k}_2 \cdot (\mathbf{x}_3 - \mathbf{x}_1)} e^{-i\mathbf{k} \cdot \mathbf{x}_3} e^{-i\mathbf{p} \cdot \mathbf{x}_1} e^{-i\mathbf{q} \cdot \mathbf{x}_2}}{[\mathbf{k}_1^2 + z_1(1 - z_1)Q^2] \left[ Q^2 + \frac{\mathbf{k}_1^2}{z_1} + \frac{\mathbf{k}_2^2}{z_3} + \frac{(\mathbf{k}_1 - \mathbf{k}_2)^2}{z_2} \right]}. \end{aligned} \quad (4)$$

where we have factored out the overall momentum (+ component only) conserving delta function  $2\pi\delta(l^+ - p^+ - q^+ - k^+)$  (not shown and hence the reason for denoting the amplitude as  $i\mathcal{M}$  rather than  $iA$  as in the figure). We have also defined  $z_1, z_2, z_3$  as fractions of the virtual photon energy carried by the quark, anti-quark and gluon respectively.  $V(\mathbf{x}_i)$  is a Wilson line in the fundamental representation, while  $U(\mathbf{x}_i)^{ba}$  is a Wilson line in the adjoint representation. The numerators  $N_i$  contain the spinor structures of the amplitude and are defined as

$$\begin{aligned} N_1 &= \frac{\bar{u}(p)\not{\epsilon}^*(k)(\not{p} + \not{k})\not{\eta}\not{k}_1\not{\epsilon}(l)(\not{k}_1 - \not{l})\not{\eta}v(q)}{16(l^+)^2(p+k)^2}, & N_2 &= \frac{\bar{u}(p)\not{\eta}(\not{l} - \not{k}_1)\not{\epsilon}(l)\not{k}_1\not{\eta}(\not{q} + \not{k})\not{\epsilon}^*(k)v(q)}{16(l^+)^2(q+k)^2}, \\ N_3 &= \frac{\bar{u}(p)\not{\eta}(\not{k}_1 - \not{k}_2)\gamma^\mu\not{k}_1\not{\epsilon}(l)(\not{l} - \not{k}_1)\not{\eta}v(q)d_{\mu\nu}(k_2)\epsilon^\nu(k)^*}{16(l^+)^2}, & N_4 &= \frac{\bar{u}(p)\not{\eta}(\not{l} - \not{k}_1)\not{\epsilon}(l)\not{k}_1\gamma^\mu(\not{k}_2 - \not{k}_1)\not{\eta}v(q)d_{\mu\nu}(k_2)\epsilon^\nu(k)^*}{16(l^+)^2}. \end{aligned} \quad (5)$$

In this exploratory work we consider a longitudinally polarized photon and use the spinor helicity formalism to evaluate these numerators for a given parton helicity. The integrals over  $\mathbf{k}_1$  and  $\mathbf{k}_2$  can then be performed. Here we show the

amplitudes for the specific case of a positive helicity quark (so that anti-quark has negative helicity) and gluon, and a longitudinally polarized photon.

$$i\mathcal{M}_1^{aL;+,+} = 8egl^+ \int d^2\mathbf{x}_1 d^2\mathbf{x}_2 t^a V(\mathbf{x}_1) V^\dagger(\mathbf{x}_2) e^{-i\mathbf{p}\cdot\mathbf{x}_1} e^{-i\mathbf{q}\cdot\mathbf{x}_2} \left[ \frac{-Q(z_1 z_2)^{\frac{3}{2}}(1-z_2)}{(2\pi)} \right] K_0(|\mathbf{x}_{12}|Q_2) \frac{e^{-i\mathbf{k}\cdot\mathbf{x}_1}}{(p+k)^2} \left( \frac{\mathbf{k}\cdot\boldsymbol{\epsilon}}{z_3} - \frac{\mathbf{p}\cdot\boldsymbol{\epsilon}}{z_1} \right). \quad (6)$$

$$i\mathcal{M}_2^{aL;+,+} = 8egl^+ \int d^2\mathbf{x}_1 d^2\mathbf{x}_2 V(\mathbf{x}_1) V^\dagger(\mathbf{x}_2) t^a e^{-i\mathbf{p}\cdot\mathbf{x}_1} e^{-i\mathbf{q}\cdot\mathbf{x}_2} \left[ \frac{Q(z_1)^{\frac{3}{2}}\sqrt{z_2}(1-z_1)^2}{(2\pi)} \right] K_0(|\mathbf{x}_{12}|Q_1) \frac{e^{-i\mathbf{k}\cdot\mathbf{x}_2}}{(q+k)^2} \left( \frac{\mathbf{k}\cdot\boldsymbol{\epsilon}}{z_3} - \frac{\mathbf{q}\cdot\boldsymbol{\epsilon}}{z_2} \right). \quad (7)$$

$$i\mathcal{M}_3^{aL;+,+} = \frac{8egl^+}{z_1} \int d^2\mathbf{x}_1 d^2\mathbf{x}_2 d^2\mathbf{x}_3 V(\mathbf{x}_1) t^b V^\dagger(\mathbf{x}_2) U(\mathbf{x}_3)_{ba} e^{-i\mathbf{p}\cdot\mathbf{x}_1} e^{-i\mathbf{q}\cdot\mathbf{x}_2} \left[ -Q(z_1 z_2)^{\frac{3}{2}}(1-z_2) \right] \frac{i}{(2\pi)^2} \frac{z_1}{1-z_2} \frac{\mathbf{x}_{31}\cdot\boldsymbol{\epsilon}}{\mathbf{x}_{31}^2} K_0(QX) e^{-i\mathbf{k}\cdot\mathbf{x}_3}. \quad (8)$$

$$i\mathcal{M}_4^{aL;+,+} = \frac{8egl^+}{z_2} \int d^2\mathbf{x}_1 d^2\mathbf{x}_2 d^2\mathbf{x}_3 V(\mathbf{x}_1) t^b V^\dagger(\mathbf{x}_2) U(\mathbf{x}_3)_{ba} e^{-i\mathbf{p}\cdot\mathbf{x}_1} e^{-i\mathbf{q}\cdot\mathbf{x}_2} \left[ Q(z_1)^{\frac{3}{2}}\sqrt{z_2}(1-z_1)^2 \right] \frac{i}{(2\pi)^2} \frac{z_2}{1-z_1} \frac{\mathbf{x}_{32}\cdot\boldsymbol{\epsilon}}{\mathbf{x}_{32}^2} K_0(QX) e^{-i\mathbf{k}\cdot\mathbf{x}_3} \quad (9)$$

where we have defined some shorthand notations,

$$X = \sqrt{z_2 z_1 \mathbf{x}_{12}^2 + z_3 z_1 \mathbf{x}_{13}^2 + z_3 z_2 \mathbf{x}_{23}^2}, \quad \mathbf{x}_{ij} = \mathbf{x}_i - \mathbf{x}_j, \quad Q_i = Q\sqrt{z_i(1-z_i)}, \quad \boldsymbol{\epsilon} = \frac{1}{\sqrt{2}}(1, i). \quad (10)$$

The next step is to square a given helicity amplitude and then to add up all the squared helicity amplitudes to get the un-polarized cross section. For example, the first helicity amplitude (6) squared and summed over final state helicities, labeled as  $\mathcal{M}_{11}^L$  is

$$\mathcal{M}_{11}^L = \frac{64e^2 g^2 Q^2 (l^+)^2 z_1 z_2^3 (1-z_2)^2 (z_1^2 + (1-z_2)^2)}{(2\pi)^2} \int d^8x \text{Tr}_c \left[ t^a (V_1 V_2^\dagger - 1) (V_2' V_1'^\dagger - 1) t^a \right] e^{i\mathbf{p}\cdot(\mathbf{x}'_1 - \mathbf{x}_1)} e^{i\mathbf{q}\cdot(\mathbf{x}'_2 - \mathbf{x}_2)} K_0(|\mathbf{x}_{12}|Q_2) K_0(|\mathbf{x}_{1'2'}|Q_2) \frac{e^{i\mathbf{k}\cdot(\mathbf{x}'_1 - \mathbf{x}_1)}}{(p+k)^4} \left( \frac{\mathbf{p}}{z_1} - \frac{\mathbf{k}}{z_3} \right)^2 \quad (11)$$

where  $d^8x$  denotes  $d^2\mathbf{x}_1 d^2\mathbf{x}_2 d^2\mathbf{x}'_1 d^2\mathbf{x}'_2$  with  $V_i \equiv V(\mathbf{x}_i)$ . To proceed further we take the soft gluon limit ( $z_3 \ll z_1, z_2$ ) and perform the integrals over the transverse momentum  $\mathbf{k}$ . We also define the two and four point functions of Wilson lines  $S^{(2)}(\mathbf{x}_i, \mathbf{x}_j)$  with shorthand  $S_{ij}$  and  $S^{(4)}(\mathbf{x}_i, \mathbf{x}_j, \mathbf{x}_k, \mathbf{x}_l)$  with shorthand  $S_{ijkl}$  (dipoles and quadrupoles) as

$$S_{ij} = \frac{1}{N_c} \text{Tr}_c \langle V(\mathbf{x}_i) V^\dagger(\mathbf{x}_j) \rangle, \quad S_{ijkl} = \frac{1}{N_c} \text{Tr}_c \langle V(\mathbf{x}_i) V^\dagger(\mathbf{x}_j) V(\mathbf{x}_k) V^\dagger(\mathbf{x}_l) \rangle. \quad (12)$$

which can be evaluated explicitly in the Gaussian approximation [10, 44–47] and are given by

$$S_{ij} = e^{-Q_s^2 \Gamma_{ij}}, \quad S_{ijkl} = S_{il} S_{jk} - \left[ \frac{\Gamma_{ij}^2 + \Gamma_{kl}^2 - \Gamma_{ik}^2 - \Gamma_{jl}^2}{\Gamma_{ij}^2 + \Gamma_{kl}^2 - \Gamma_{il}^2 - \Gamma_{jk}^2} \right] (S_{il} S_{jk} - S_{ij} S_{kl}), \quad \Gamma_{ij} = (\mathbf{x}_i - \mathbf{x}_j)^2 \log \frac{1}{\Lambda |\mathbf{x}_i - \mathbf{x}_j|}. \quad (13)$$

where  $\Lambda$  is an infrared regulator. The presence of the logarithm in  $\Gamma_{ij}$  is essential for the correct power-law behavior of the cross sections at high transverse momenta. However it does make the analytic evaluation of these integrals impossible. As we will be exploring the more interesting (and experimentally accessible) region of low to intermediate transverse momenta we will ignore it in this exploratory study which corresponds to taking the Golec Biernat-Wusthoff model [48] of the dipole profile. With these approximations our full amplitude squared for production of a quark, anti-quark and a gluon with the transverse momentum of the gluon integrated can be written as

$$\begin{aligned}
\int \frac{d^2\mathbf{k}}{(2\pi)^2} |i\mathcal{M}|^2 &= \int \frac{d^2\mathbf{k}}{(2\pi)^2} \left[ \mathcal{M}_{11}^L + \mathcal{M}_{22}^L + \mathcal{M}_{33}^L + \mathcal{M}_{44}^L + 2\mathcal{M}_{12}^L + 2\mathcal{M}_{13}^L + 2\mathcal{M}_{14}^L + 2\mathcal{M}_{23}^L + 2\mathcal{M}_{24}^L + 2\mathcal{M}_{34}^L \right] \\
&= \frac{64e^2 g^2 Q^2 (l^+)^2 N_c^2 (z_1 z_2)^3}{(2\pi)^4} \int d^{10}x K_0(|\mathbf{x}_{12}|Q_1) K_0(|\mathbf{x}_{1'2'}|Q_1) e^{i\mathbf{p}\cdot(\mathbf{x}'_1 - \mathbf{x}_1)} e^{i\mathbf{q}\cdot(\mathbf{x}'_2 - \mathbf{x}_2)} \\
&\quad \left\{ [S_{122'1'} - S_{12} - S_{1'2'} + 1] \left( \Delta_{11'}^{(3)} + \Delta_{22'}^{(3)} \right) \right. \\
&\quad + [S_{11'} S_{22'} - S_{23} S_{13} - S_{2'3} S_{1'3} + 1] \left( \Delta_{11'}^{(3)} + \Delta_{22'}^{(3)} - 2\Delta_{12'}^{(3)} \right) \\
&\quad - [S_{12} S_{1'2'} - S_{12} - S_{1'2'} + 1] 2\Delta_{12'}^{(3)} \\
&\quad + [S_{122'3} S_{1'3} - S_{2'3} S_{1'3} - S_{12} + 1] \left( 2\Delta_{11'}^{(3)} - 2\Delta_{12'}^{(3)} \right) \\
&\quad \left. + [S_{1231'} S_{2'3} - S_{2'3} S_{1'3} - S_{12} + 1] \left( 2\Delta_{22'}^{(3)} - 2\Delta_{21'}^{(3)} \right) \right\}. \tag{14}
\end{aligned}$$

with the radiation kernel  $\Delta_{ij}^{(3)}$  given by

$$\Delta_{ij}^{(3)} = \frac{(\mathbf{x}_3 - \mathbf{x}_i) \cdot (\mathbf{x}_3 - \mathbf{x}_j)}{(\mathbf{x}_3 - \mathbf{x}_i)^2 (\mathbf{x}_3 - \mathbf{x}_j)^2}. \tag{15}$$

While this result looks very compact it is still not very amenable to phenomenological studies of importance to experiments. Therefore we consider the more interesting limit of back-to-back azimuthal angular correlations.

### III. THE BACK-TO-BACK LIMIT OF AZIMUTHAL ANGULAR CORRELATIONS

To make a quantitative estimate of the role of coherent energy loss and gluon saturation we will focus on the back-to-back kinematics region in dihadron production in DIS at small  $x$ . To this end we define the total and relative momenta

$$\mathbf{P} \equiv \mathbf{p} + \mathbf{q}, \quad \mathbf{K} \equiv z_2 \mathbf{p} - z_1 \mathbf{q}. \tag{16}$$

and take the "back-to-back correlation" limit [45, 49] defined as

$$|\mathbf{P}| \ll |\mathbf{K}| \sim |\mathbf{p}| \sim |\mathbf{q}| \tag{17}$$

We define new coordinate-space variables,  $\mathbf{u}, \mathbf{v}, \mathbf{u}', \mathbf{v}'$ ,

$$\mathbf{u} = \mathbf{x}_1 - \mathbf{x}_2, \quad \mathbf{v} = z_1 \mathbf{x}_1 + z_2 \mathbf{x}_2, \quad \mathbf{u}' = \mathbf{x}'_1 - \mathbf{x}'_2, \quad \mathbf{v}' = z_1 \mathbf{x}'_1 + z_2 \mathbf{x}'_2. \tag{18}$$

in terms of which the back-to-back limit corresponds to taking  $|\mathbf{u}| \sim |\mathbf{u}'| \ll 1$ . Taking this limit in (14) and expanding to lowest nonzero order in  $\mathbf{u}$  and  $\mathbf{u}'$  we get

$$\begin{aligned}
\int \frac{d^2\mathbf{k}}{(2\pi)^2} |i\mathcal{M}|^2 &= \frac{64e^2 g^2 Q^2 (l^+)^2 N_c^2 (z_1 z_2)^3}{(2\pi)^4} \pi R^2 \int d^2\mathbf{u} d^2\mathbf{u}' d^2\mathbf{v} d^2\mathbf{v}' K_0(Q_1|\mathbf{u}|) K_0(Q_1|\mathbf{u}'|) e^{i\mathbf{P}\cdot(\mathbf{v}' - \mathbf{v})} e^{i\mathbf{K}\cdot(\mathbf{u}' - \mathbf{u})} \\
&\quad \left[ \frac{(1 - e^{-2Q_s^2(\mathbf{v} - \mathbf{v}')^2}) [\mathbf{v}^2 + \mathbf{v}'^2 - (\mathbf{v} - \mathbf{v}')^2] \mathbf{u} \cdot \mathbf{u}'}{(\mathbf{v} - \mathbf{v}')^2 \mathbf{v}^2 \mathbf{v}'^2} \right. \\
&\quad + \frac{4e^{-2Q_s^2 \mathbf{v}^2} \left( 1 - e^{-2Q_s^2(\mathbf{v}^2 - \mathbf{v} \cdot \mathbf{v}')} \right) (\mathbf{u} \cdot \mathbf{v}') [2(\mathbf{v} \cdot \mathbf{v}')(\mathbf{u}' \cdot \mathbf{v}') - (\mathbf{u}' \cdot \mathbf{v}) \mathbf{v}'^2]}{\mathbf{v}^2 \mathbf{v}'^4 (\mathbf{v}^2 - \mathbf{v} \cdot \mathbf{v}')} \\
&\quad \left. + \frac{\left( 1 + e^{-2Q_s^2(\mathbf{v} - \mathbf{v}')^2} - e^{-2Q_s^2 \mathbf{v}^2} - e^{-2Q_s^2 \mathbf{v}'^2} \right)}{\mathbf{v}^4 \mathbf{v}'^4} [4(\mathbf{u} \cdot \mathbf{v})(\mathbf{u}' \cdot \mathbf{v}')(\mathbf{v} \cdot \mathbf{v}') - 4(\mathbf{u} \cdot \mathbf{v}')(\mathbf{u}' \cdot \mathbf{v}) \mathbf{v}^2 + (\mathbf{u} \cdot \mathbf{u}') \mathbf{v}^2 \mathbf{v}'^2] \right] \tag{19}
\end{aligned}$$

where  $\pi R^2$  is the transverse area of the target arising from integration over  $\mathbf{x}_3$  (after a substitution). The integrals over  $\mathbf{u}$  and  $\mathbf{u}'$  can now be evaluated explicitly and the remaining integrals over  $\mathbf{v}$  and  $\mathbf{v}'$  integrals can be written in polar coordinates to get

$$\int \frac{d^2\mathbf{k}}{(2\pi)^2} |i\mathcal{M}|^2 = \frac{64e^2 g^2 Q^2 (l^+)^2 N_c^2 (z_1 z_2)^3}{(2\pi)^2} \frac{4\pi R^2 K^2}{(K^2 + Q_1^2)^4} \int dr dr' d\phi d\phi' e^{i\frac{P}{\Lambda} r' \cos(\phi' - \phi_P)} e^{-i\frac{P}{\Lambda} r \cos(\phi - \phi_P)} \left[ 2 \frac{(1 - e^{-2\frac{Q_s}{\Lambda}(r^2 + r'^2 - 2rr' \cos(\phi - \phi'))}) \cos(\phi - \phi')}{r^2 + r'^2 - 2rr' \cos(\phi - \phi')} + \frac{4e^{-2\frac{Q_s}{\Lambda} r'^2} (1 - e^{-2\frac{Q_s}{\Lambda}(r^2 - rr' \cos(\phi - \phi'))}) \cos(\phi') [2 \cos(\phi - \phi') \cos(\phi') - \cos(\phi)]}{r^2 - rr' \cos(\phi - \phi')} + \frac{(1 + e^{-2\frac{Q_s}{\Lambda}(r^2 + r'^2 - 2rr' \cos(\phi - \phi'))} - e^{-2\frac{Q_s}{\Lambda} r^2} - e^{-2\frac{Q_s}{\Lambda} r'^2})}{rr'} [4 \cos(\phi) \cos(\phi') \cos(\phi - \phi') - 4 \cos^2(\phi') + 1] \right] \quad (20)$$

where we have defined new dimensionless variables  $r$  and  $r'$

$$r = \Lambda |\mathbf{v}|, \quad r' = \Lambda |\mathbf{v}'| \quad (21)$$

and  $\Lambda$  is a constant parameter with units of mass. All angles are measured relative to the  $\mathbf{K}$  vector so that  $\phi_P$  is the angle between  $\mathbf{P}$  and  $\mathbf{K}$ , and  $(\phi, \phi')$  are the angles of  $(\mathbf{v}, \mathbf{v}')$  with respect to  $\mathbf{K}$ .

We calculate the medium-induced, coherent energy loss as defined in (2). The induced radiation spectrum can be written as,

$$z_3 \frac{dI_{\text{ind}}}{dz_3} = \frac{2\alpha_s N_c}{(2\pi)^3} \left[ \frac{\int dr dr' d\phi d\phi' f(r, r', \phi, \phi')}{\int \frac{dr}{r} J_0\left(\frac{P}{\Lambda} r\right) \left(1 - e^{-2\frac{Q_s}{\Lambda} r^2}\right)} \Big|_A - \frac{\int dr dr' d\phi d\phi' f(r, r', \phi, \phi')}{\int \frac{dr}{r} J_0\left(\frac{P}{\Lambda} r\right) \left(1 - e^{-2\frac{Q_s}{\Lambda} r^2}\right)} \Big|_p \right]. \quad (22)$$

Here  $f(r, r', \phi, \phi')$  is the integrand in Eq. 20 and the Leading Order result [4] is used in the denominator. The only difference between the first and second terms is the different saturation scale  $Q_s$  of a nucleus and a proton. It should be noted that we have taken the same back-to-back limit in the denominators above which describe the Leading Order quark anti-quark production cross sections. Furthermore, we use a cut off on the integration variables  $r$  and  $r'$  in order to impose color neutrality at scales comparable to confinement scale  $\Lambda_{QCD}$  (i.e. we choose  $\Lambda = \Lambda_{QCD} = 200\text{MeV}$  and the  $r, r'$  integrals then go from 0 to 1). Finally, to get an estimate of the energy loss effects we consider some specific values for the final state partons; we will consider the case when both partons have similar rapidities so that  $z_1 = 0.55, z_2 = 0.45$  and their transverse momenta are of the order of the photon virtuality  $Q$ , specifically

$$|\mathbf{p}| = Q \quad |\mathbf{q}| = Q + 0.1 \text{ GeV}, \quad Q_{s,p}^2 = 1 \text{ GeV}^2, \quad Q_{s,A}^2 = A^{1/3} Q_{s,p}^2. \quad (23)$$

We show our results for the medium-induced coherent energy loss (22) in Fig.(2) for various values of external momenta, and two different values of nuclear saturation scale which mimics changing centrality, rapidity and/or nuclear  $A$  number.

As seen the induced radiation is largest at the back to back kinematics and drops off sharply as one goes away from this limit. Also at the exact back to back limit the induced radiation is independent of photon virtuality, this is so since we have taken the quark and anti-quark momenta equal to photon virtuality. Furthermore the size of induced radiation increases with nuclear size as expected. This is also indicative of the size of the Next to Leading Order corrections, however keeping in mind that contributions of some of the Next to Leading terms cancel between a proton and a nucleus target in our definition of energy loss radiation spectrum in (2). This clearly shows the importance of the full Next to Leading Order corrections to dihadron production cross section in DIS at small  $x$ . This is work in progress and will be reported elsewhere [27]. Another effect that is known to be important is the Sudakov effect [18, 50], however this is beyond the scope of this work and will not be considered here.

To implement the cold matter energy loss effects in dihadron angular correlations, we calculate the coincidence probability (3) using numerical methods to evaluate the remaining integrals. Following [13], we choose similar values

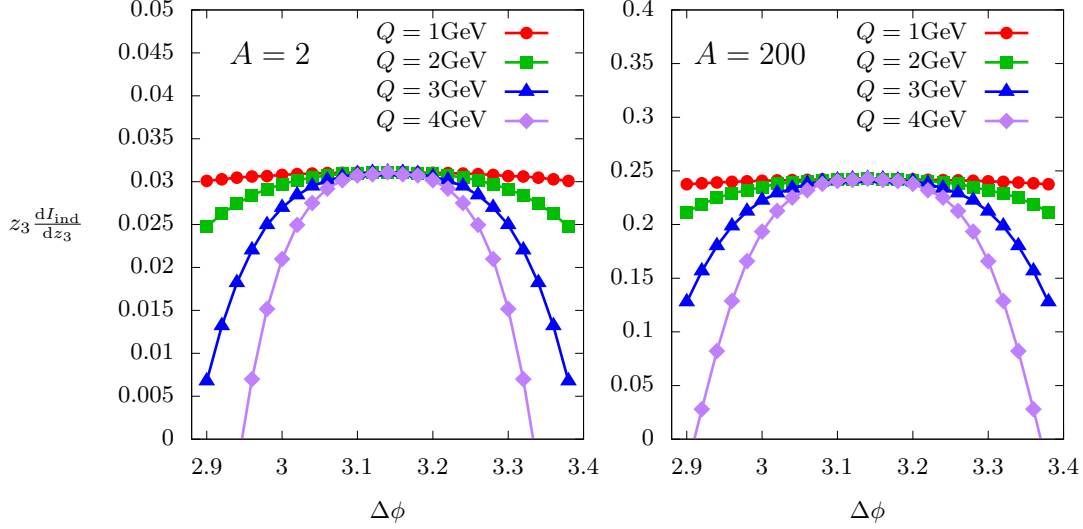


FIG. 2: The induced radiation spectrum plotted for  $A = 2$  and  $A = 200$  at four different values of  $Q$ . Note that we maintain  $|\mathbf{p}| = Q$  and  $|\mathbf{q}| = Q + 0.1\text{GeV}$  and that the vertical scales in the two graphs are different.

for the external momentum windows, we choose  $p_{\min} = 2\text{ GeV}$ ,  $p_{\max} = 10\text{ GeV}$ ,  $q_{\min} = 1\text{ GeV}$ ,  $q_{\max} = p$ . We also impose color neutrality at lengths beyond 1fm by using a cutoff on the  $r, r'$  integrals by choosing  $\Lambda = \Lambda_{QCD} = 0.2\text{ GeV}$  and setting  $r_{\max} = 1$ . We fix the rapidities by choosing  $z_1 = 0.55$ ,  $z_2 = 0.45$ . We use the back-to-back limit in both  $N_{\text{pair}}$  and in the single inclusive  $N_{\text{trig}}$ <sup>3</sup>.

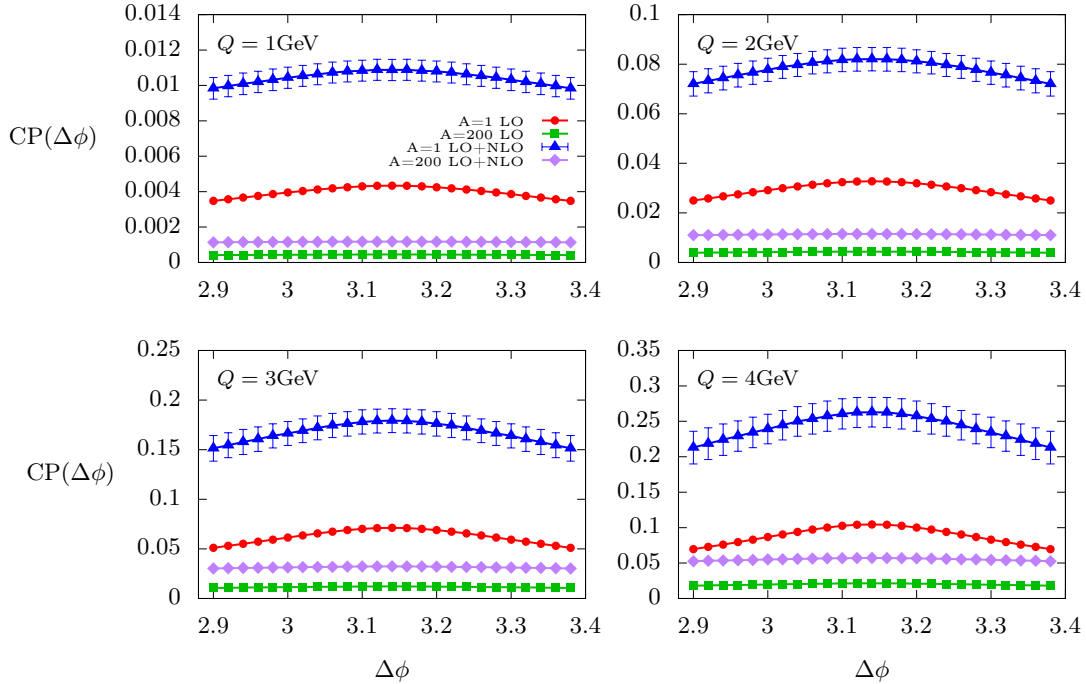


FIG. 3: The effect of Next to Leading order corrections on the coincidence probability  $\text{CP}(\Delta\phi)$ , shown for four different values of photon virtuality  $Q$  for a proton target ( $A = 1$ ) and a large nuclear target ( $A = 200$ ).

<sup>3</sup> We are grateful to C. Marquet for emphasizing this point to us.

Clearly the induced radiation which is "lost" has a significant effect on the away side peak of dihadron azimuthal angular correlations. Note that we have restricted ourselves to angles in a very narrow window around the away side hadron. This is due to our strict back to back approximation which is expected to break down when going away from the away side hadron by a large angle. A proper quantitative estimate of the size of these corrections to the back to back approximation requires a detailed quantitative study using the various improved Transverse Momentum Dependent (TMD) distributions as advocated in [51, 52] and in [53–58] for proton-nucleus collisions. Nevertheless for the sake of comparison we show our results for a much wider range in  $\Delta\phi$  once in Fig. (4) and limit the rest of our analysis to the range  $\Delta\phi \in [2.9, 3.4]$  where we expect that the back-to-back approximation will still provide accurate results.

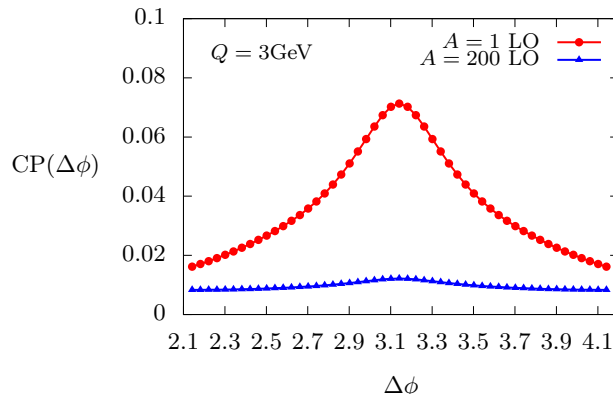


FIG. 4:  $CP(\Delta\phi)$  calculated at leading order using the back-to-back approximation in both  $N_{\text{pair}}$  and  $N_{\text{pair}}$  with a wider angle window  $\Delta\phi \in [\pi - 1, \pi + 1]$  for the case  $Q = 3\text{GeV}$ .

To see the effect of the "lost" radiation more clearly we show the ratio of coincidence probabilities with the induced radiation to that of no radiation in Fig.(5) where an enhancement factor of order 3 is seen with a weak angular dependence .

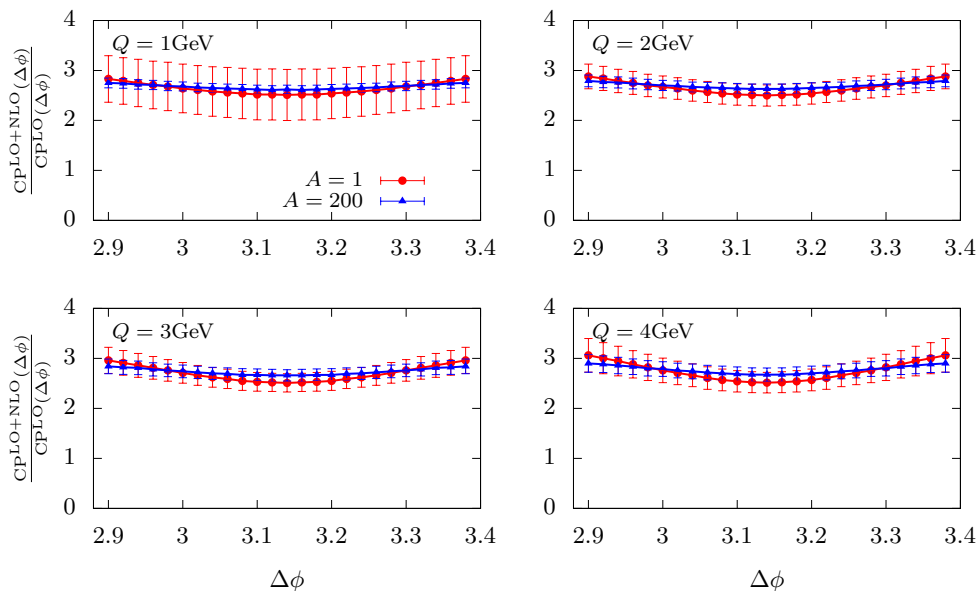


FIG. 5: Here we show the ratio of  $CP(\Delta\phi)$  at next-to-leading order versus at leading order calculated for a proton and a large nucleus target. A very weak dependence of next to leading order corrections on target size and angle is observed for small angles away from  $\pi$ .



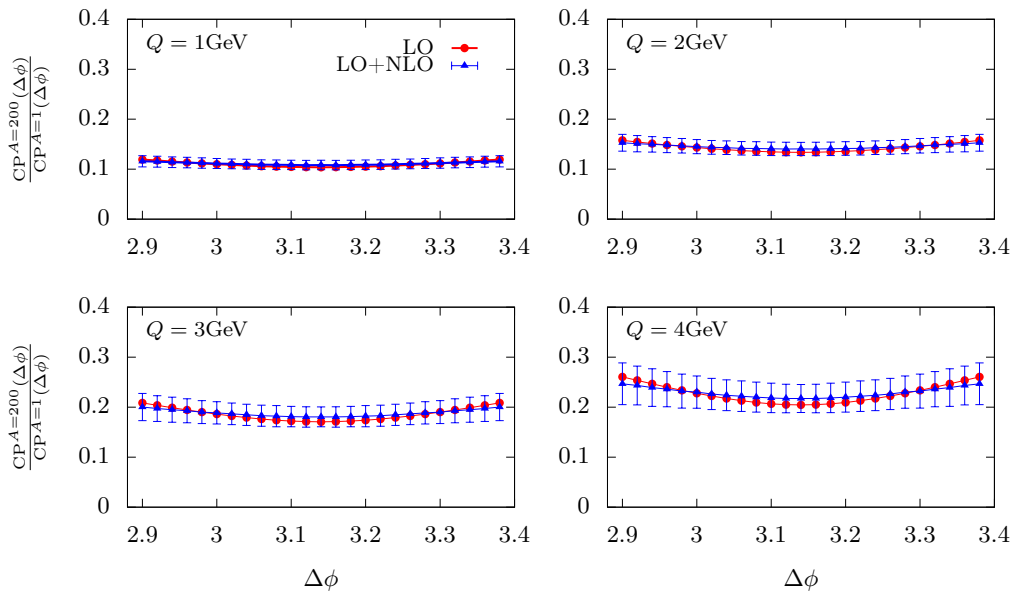


FIG. 6: The double ratio of  $CP(\Delta\phi)$  for a large nucleus over the  $CP(\Delta\phi)$  for a proton, calculated at leading order and at next-to-leading order.

To investigate the medium dependence of the coincidence probability we define the double ratio of coincidence probabilities for a nucleus vs a proton in analogy with the medium modification factor  $R_{pA}$  in proton-nucleus collisions and show this double ratio in Fig.(6). A significant reduction of the coincidence probability for a nucleus target is seen which is again very robust against next to leading order corrections. A clear increase in the magnitude of this double ratio is seen with the increasing photon virtuality, reminiscent of the behavior of  $R_{pA}$  in proton-nucleus collisions.

There are several ways in which our exploratory study can be improved; we have used the GBW model of dipole profile which is known to miss the high  $p_t$  tail of the production spectra. One can improve the calculation by using more realistic dipole profiles which have become available recently. It will also be important to go beyond the strict back to back limit so that one can extend the present analysis to larger angles away from  $\pi$ . This will also shed light on the domain of applicability of back to back approximation. Furthermore, we have only considered longitudinal photons, in a more realistic analysis one will need to include transverse photons as well. However we do not expect our results to change much by this. Lastly, we have considered the effect of radiated soft gluon on the quark anti-quark production by integrating out the radiated gluon. In a more realistic approach to dihadron production one will need to consider integrating out any of the three outgoing partons. This will be done when we compute the full next to leading order corrections to dihadron production and express (some of) the final state singularities into hadron fragmentation functions. This is work in progress and will be reported elsewhere [27].

In summary we have performed an exploratory study of the contribution of coherent, medium-induced radiative energy loss to the away-side peak in dihadron azimuthal angular correlations in DIS at small  $x$ . We observe a sizable contribution to the coincidence probability from the induced radiation which indicates the significance of next to leading order corrections to dihadron azimuthal angular correlations. We have defined a double ratio of coincidence probabilities and have shown that it is very stable against higher order corrections and thus may be a more robust signature of saturation dynamics.

#### ACKNOWLEDGMENTS

We gratefully acknowledge support from the DOE Office of Nuclear Physics through Grant No. DE-SC0002307 and by PSC-CUNY through grant No. 63158-0051. We would like to thank F. Arleo, E. Aschenauer, G. Beuf, F. Gelis, K. Fukushima, T. Lappi, R. Venugopalan, B. Xiao and especially C. Marquet, S. Munier and S. Peigné for helpful discussions.

---

[1] F. D. Aaron et al. (H1), Eur. Phys. J. C **64**, 561 (2009), 0904.3513.

- [2] L. V. Gribov, E. M. Levin, and M. G. Ryskin, Phys. Rept. **100**, 1 (1983).
- [3] A. H. Mueller and J.-w. Qiu, Nucl. Phys. B **268**, 427 (1986).
- [4] F. Gelis, E. Iancu, J. Jalilian-Marian, and R. Venugopalan, Ann. Rev. Nucl. Part. Sci. **60**, 463 (2010), 1002.0333.
- [5] L. D. McLerran and R. Venugopalan, Phys. Rev. D **49**, 2233 (1994), hep-ph/9309289.
- [6] J. Jalilian-Marian, A. Kovner, L. D. McLerran, and H. Weigert, Phys. Rev. D **55**, 5414 (1997), hep-ph/9606337.
- [7] J. L. Albacete et al., Nucl. Phys. A **972**, 18 (2018), 1707.09973.
- [8] E.-C. Aschenauer et al. (2016), 1602.03922.
- [9] A. Accardi et al., Eur. Phys. J. A **52**, 268 (2016), 1212.1701.
- [10] J. Jalilian-Marian and Y. V. Kovchegov, Phys. Rev. D **70**, 114017 (2004), [Erratum: Phys.Rev.D 71, 079901 (2005)], hep-ph/0405266.
- [11] J. Jalilian-Marian, Nucl. Phys. A **770**, 210 (2006), hep-ph/0509338.
- [12] C. Marquet, Nucl. Phys. A **796**, 41 (2007), 0708.0231.
- [13] J. L. Albacete and C. Marquet, Phys. Rev. Lett. **105**, 162301 (2010), 1005.4065.
- [14] A. Stasto, B.-W. Xiao, and F. Yuan, Phys. Lett. B **716**, 430 (2012), 1109.1817.
- [15] T. Lappi and H. Mantysaari, Nucl. Phys. A **908**, 51 (2013), 1209.2853.
- [16] J. Jalilian-Marian and A. H. Rezaeian, Phys. Rev. D **86**, 034016 (2012), 1204.1319.
- [17] J. Jalilian-Marian and A. H. Rezaeian, Phys. Rev. D **85**, 014017 (2012), 1110.2810.
- [18] L. Zheng, E. C. Aschenauer, J. H. Lee, and B.-W. Xiao, Phys. Rev. D **89**, 074037 (2014), 1403.2413.
- [19] A. Stasto, S.-Y. Wei, B.-W. Xiao, and F. Yuan, Phys. Lett. B **784**, 301 (2018), 1805.05712.
- [20] J. L. Albacete, G. Giacalone, C. Marquet, and M. Matas, Phys. Rev. D **99**, 014002 (2019), 1805.05711.
- [21] H. Mäntysaari, N. Mueller, F. Salazar, and B. Schenke, Phys. Rev. Lett. **124**, 112301 (2020), 1912.05586.
- [22] Y. Hatta, B.-W. Xiao, F. Yuan, and J. Zhou, Phys. Rev. Lett. **126**, 142001 (2021), 2010.10774.
- [23] J. Jia, S.-Y. Wei, B.-W. Xiao, and F. Yuan, Phys. Rev. D **101**, 094008 (2020), 1910.05290.
- [24] E. Braidot (STAR), Nucl. Phys. A **854**, 168 (2011), 1008.3989.
- [25] A. Adare et al. (PHENIX), Phys. Rev. Lett. **107**, 172301 (2011), 1105.5112.
- [26] Z.-B. Kang, I. Vitev, and H. Xing, Phys. Rev. D **85**, 054024 (2012), 1112.6021.
- [27] F. Bergabo and J. Jalilian-Marian (2021), in progress.
- [28] P. Caucal, F. Salazar, and R. Venugopalan (2021), 2108.06347.
- [29] A. Ayala, M. Hentschinski, J. Jalilian-Marian, and M. E. Tejeda-Yeomans, Phys. Lett. B **761**, 229 (2016), 1604.08526.
- [30] A. Ayala, M. Hentschinski, J. Jalilian-Marian, and M. E. Tejeda-Yeomans, Nucl. Phys. B **920**, 232 (2017), 1701.07143.
- [31] F. Gelis and J. Jalilian-Marian, Phys. Rev. D **67**, 074019 (2003), hep-ph/0211363.
- [32] I. Balitsky, Nucl. Phys. B **463**, 99 (1996), hep-ph/9509348.
- [33] Y. V. Kovchegov, Phys. Rev. D **61**, 074018 (2000), hep-ph/9905214.
- [34] J. Jalilian-Marian, A. Kovner, A. Leonidov, and H. Weigert, Nucl. Phys. B **504**, 415 (1997), hep-ph/9701284.
- [35] J. Jalilian-Marian, A. Kovner, A. Leonidov, and H. Weigert, Phys. Rev. D **59**, 014014 (1998), hep-ph/9706377.
- [36] J. Jalilian-Marian, A. Kovner, and H. Weigert, Phys. Rev. D **59**, 014015 (1998), hep-ph/9709432.
- [37] A. Kovner, J. G. Milhano, and H. Weigert, Phys. Rev. D **62**, 114005 (2000), hep-ph/0004014.
- [38] E. Iancu, A. Leonidov, and L. D. McLerran, Nucl. Phys. A **692**, 583 (2001), hep-ph/0011241.
- [39] E. Ferreira, E. Iancu, A. Leonidov, and L. McLerran, Nucl. Phys. A **703**, 489 (2002), hep-ph/0109115.
- [40] A. Dumitru, J. Jalilian-Marian, T. Lappi, B. Schenke, and R. Venugopalan, Phys. Lett. B **706**, 219 (2011), 1108.4764.
- [41] A. Dumitru, J. Jalilian-Marian, and E. Petreska, Phys. Rev. D **84**, 014018 (2011), 1105.4155.
- [42] A. Dumitru and J. Jalilian-Marian, Phys. Rev. D **82**, 074023 (2010), 1008.0480.
- [43] S. Munier, S. Peigné, and E. Petreska, Phys. Rev. D **95**, 014014 (2017), 1603.01028.
- [44] J. P. Blaizot, F. Gelis, and R. Venugopalan, Nucl. Phys. A **743**, 57 (2004), hep-ph/0402257.
- [45] F. Dominguez, C. Marquet, B.-W. Xiao, and F. Yuan, Phys. Rev. D **83**, 105005 (2011), 1101.0715.
- [46] K. Fukushima and Y. Hidaka, JHEP **11**, 114 (2017), 1708.03051.
- [47] T. Lappi, H. Mäntysaari, and A. Ramnath, Phys. Rev. D **102**, 074027 (2020), 2007.00751.
- [48] K. J. Golec-Biernat and M. Wusthoff, Phys. Rev. D **59**, 014017 (1998), hep-ph/9807513.
- [49] F. Dominguez, B.-W. Xiao, and F. Yuan, Phys. Rev. Lett. **106**, 022301 (2011), 1009.2141.
- [50] A. H. Mueller, B.-W. Xiao, and F. Yuan, Phys. Rev. Lett. **110**, 082301 (2013), 1210.5792.
- [51] T. Altinoluk and R. Boussarie, JHEP **10**, 208 (2019), 1902.07930.
- [52] R. Boussarie, H. Mäntysaari, F. Salazar, and B. Schenke (2021), 2106.11301.
- [53] P. Kotko, K. Kutak, C. Marquet, E. Petreska, S. Sapeta, and A. van Hameren, JHEP **09**, 106 (2015), 1503.03421.
- [54] A. van Hameren, P. Kotko, K. Kutak, C. Marquet, E. Petreska, and S. Sapeta, JHEP **12**, 034 (2016), [Erratum: JHEP 02, 158 (2019)], 1607.03121.
- [55] T. Altinoluk, R. Boussarie, and P. Kotko, JHEP **05**, 156 (2019), 1901.01175.
- [56] R. Boussarie and Y. Mehtar-Tani, Phys. Rev. D **103**, 094012 (2021), 2001.06449.
- [57] H. Fujii, C. Marquet, and K. Watanabe, JHEP **12**, 181 (2020), 2006.16279.
- [58] T. Altinoluk, C. Marquet, and P. Tael, JHEP **06**, 085 (2021), 2103.14495.